Pure & Appl. Chem., Vol. 57, No. 2, pp. 181–185, 1985.
Printed in Great Britain.

Allowed and forbidden scattering by LO phonons: interference effects

J. Menéndez and M. Cardona

Max-Planck-Institut für Festkörperforschung, Heisenbergstrasse 1,
D - 7000 Stuttgart 80, Federal Republic of Germany

Abstract - We discuss resonant scattering by LO phonons in zincblende-type semiconductors. It has an allowed (deformation potential) and a forbidden (Fröhlich interaction) component. For a (001) surface the scattering amplitude changes sign in going from the [110] to the [1$\bar{1}$0] polarized scattering configurations. The forbidden component, always diagonal, remains the same. Interference between the two components, which can be easily identified by going from the [011] to the [01$\bar{1}$] polarized configurations, takes place. These interference phenomena decrease for impure samples as a result of the incoherent forbidden scattering induced by the impurities. Data for GaAs and InSb are presented.

1. INTRODUCTION

The [110] and the [1$\bar{1}$0] directions are equivalent in the germanium structure: one is transformed into the other by a S_4 ($\equiv IC_4$) symmetry operation. This is no longer the case for the zincblende structure in which the III-V semiconductors GaAs and InSb crystallize. The inequivalence of these two directions manifests itself in a number of phenomena, for instance the first order electrooptic effect: a field along [110] produces an effect of the opposite sign to that of a field along [1$\bar{1}$0]. Recent spin-polarized photoemission experiments in GaAs (Ref. 1) also reveal the difference in symmetry between the germanium and the zincblende structures. The non-equivalent [110] and [1$\bar{1}$0] directions may be determined by inspection of the etch patterns obtained by etching zincblende materials with suitable chemicals (Ref. 2). The labelling [110] and [1$\bar{1}$0], however, depends on the choice of coordinates. It reverses when we permute the two atoms in the unit cell.

We present in this paper another effect of the [110]-[1$\bar{1}$0] inequivalence. The Raman-cross section for LO-phonons in the backscattering geometry at the (001) face is shown to have different values, depending on whether incident and scattered light are polarized parallel to [110] or to [1$\bar{1}$0]. The phenomenon, which is only observed for laser frequencies near interband critical points (Refs. 3 and 4), is due to interference of two scattering channels, the standard dipole-allowed channel and a forbidden channel due to the q-dependence of the Raman polarizability.

Our measurements were performed in GaAs, for laser frequencies near the $E_0+\Delta_0$ gap (1.849 eV at 100 K). Similar effects were seen for the E_1 gap of InSb (1.98 eV at 100 K). The allowed Raman tensors of these materials and their resonance behavior near the gaps under consideration are known (Refs. 5-7). The theory of forbidden LO-scattering induced by the Fröhlich interaction has been formulated by Martin (Ref. 8) and Zeyher, Ting, and Birman (Ref. 9). The relative sign of the allowed and forbidden contribution changes by rotating the light polarization vector from [110] to [1$\bar{1}$0]. Using the tensors given in Refs. 5-9 we can calculate the scattered intensity. The results show interference effects which are much stronger than the observed ones. We attribute this discrepancy to the fact that part of the observed forbidden LO-scattering is induced by impurities, in which case it does not interfere with the allowed LO-scattering. A much better agreement between theory and experiment is obtained by introducing the impurity contribution in the calculation of the resonant cross section.

2. RESONANCE SCATTERING BY PHONONS IN GaAs

The scattering efficiency per unit length and unit solid angle for light scattering by optical phonons is given by Eq. (2.134a) of Ref. 6:

$$\left(\frac{\partial S}{\partial \Omega}\right) = \left(\frac{\omega_S}{c}\right)^4 \frac{N\hbar}{2M^*\Omega_{opt}} |\hat{e}_S \cdot \overleftrightarrow{R} \cdot \hat{e}_L|^2 (1+n), \qquad (1)$$

where ω_S is the scattered frequency, c the speed of light, N the number of primitive cells per unit volume, M* the reduced mass of the unit cell, Ω_{opt} the optical phonon frequency, $\hat{e}_i$ ($\hat{e}_S$) the polarization vector of the incident (scattered) radiation, n the Bose-Einstein factor, and $\overleftrightarrow{R}$ the Raman tensor, whose independent component is the so-called "Raman polarizability" a.

The Raman tensor $\overleftrightarrow{R}$ can be calculated by third-order perturbation theory. Fig. 1a shows one of the contributing diagrams. The incident photon ω_L creates an exciton (electron-hole pair)

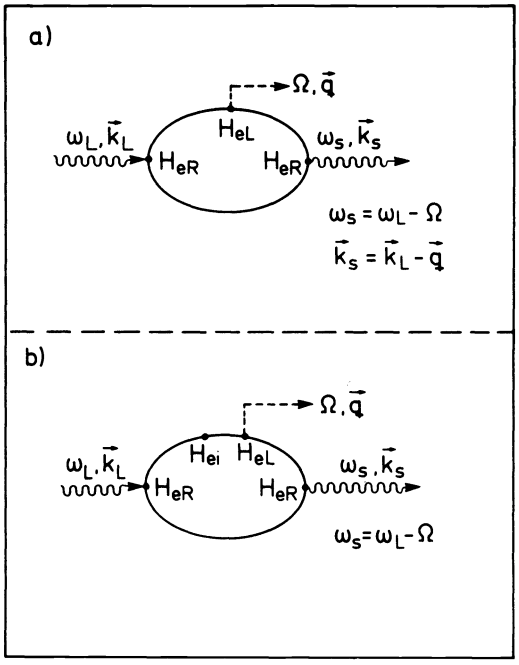

Fig. 1. a) One of the diagrams leading to first-order-Raman scattering. H_{eR} (H_{eL}) is the electron-radiation (-phonon) interaction.
b) Diagram contributing to impurity-induced Raman scattering. H_{ei} is the electron-impurity scattering Hamiltonian.

which is scattered by the electron-phonon interaction, creating a phonon of frequency Ω. The recombination of the exciton produces the scattered photon ω_S. The electron-phonon interaction H_{eL} may be written as

$$H_{eL} = H_{DP} + H_F. \tag{2}$$

H_{DP} represents the so-called deformation potential interaction, and H_F the Fröhlich interaction, which appears for longitudinal optical phonons due to the electric field produced by them. The Hamiltonian H_F has interband matrix elements (known as the electrooptic interaction) and q-dependent interband matrix elements, which lead to forbidden LO-scattering. The interband part of H_F produces essentially a renormalization of the deformation potential contribution. The corresponding tensor in this case is

$$\overleftrightarrow{R} = \begin{pmatrix} 0 & a & 0 \\ a & 0 & 0 \\ 0 & 0 & 0 \end{pmatrix} \tag{3}$$

for backscattering at a (001) surface of a zincblende-type material.

The dependence of a on photon energy ω_L is shown for GaAs in Fig. 1 of Ref. 5. The polarizability resonates strongly at the lowest direct gap E_0 and at the E_1 gaps. A weak singularity is found at the spin-orbit partner of E_0: the $E_0+\Delta_0$ gap. At this gap (between the second highest valence band Γ_7 and the lowest conduction band Γ_6), the resonance is weak because H_{DP} does not have diagonal matrix elements at Γ_7 and Γ_6.

The intraband matrix elements of H_F produce strong q-dependent (dipole-forbidden) scattering, which resonates near all direct gaps. The Raman tensor is now

$$R = \begin{pmatrix} a_F & o & o \\ o & a_F & o \\ o & o & a_F \end{pmatrix}. \tag{4}$$

For the $E_o+\Delta_o$ gap, a_F is

$$a_F \propto iq\,[(\omega_o - \omega_L - i\eta)^{1/2} - (\omega_o - \omega_S - i\eta)^{1/2}]^3 . \tag{5}$$

Using Eqs. (3) and (4) we find

$$\frac{\partial S}{\partial \Omega} \propto \begin{cases} |a+a_F|^2 \text{ for } \hat{e}_L \| \hat{e}_S \| [110] \\ |a-a_F|^2 \text{ for } \hat{e}_L \| \hat{e}_S \| [1\bar{1}0] \\ |a_F|^2 \text{ for } \hat{e}_L \| \hat{e}_S \| [100] \end{cases} \tag{6}$$

Hence, if

$$|a| \simeq |a_F| , \tag{7}$$

the scattering efficiencies for the [110] and [1$\bar{1}$0] configurations become different. This phenomenon has been recently observed for ω_L near the $E_o+\Delta_o$ gap of GaAs (Ref. 4).

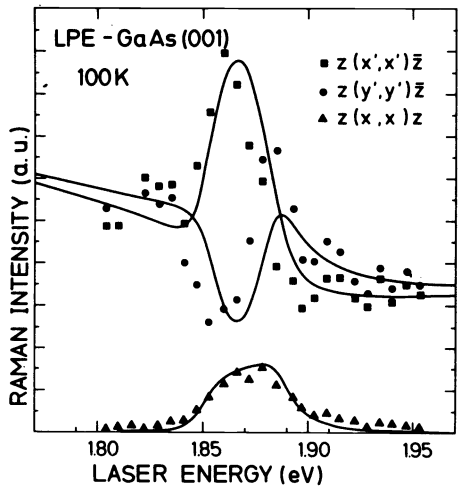

Fig. 2

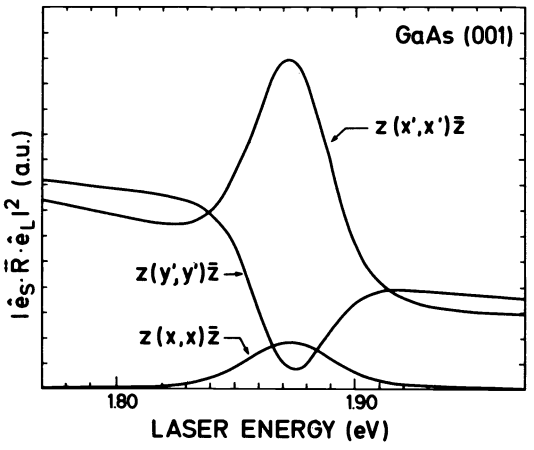

Fig. 3

Fig. 2. Experimental Raman x||[100] efficiency for the different scattering configurations in (001)-GaAs. x'||[110], y'||[1$\bar{1}$0],z||[001]. The coordinate system is chosen with the Ga-atom at the origin. The lines show the theoretical calculation with Eq. (8).

Fig. 3. Theoretical calculation of the scattering efficiency for the three configurations of Fig. 2, using Eq. (6). The broadening parameter is η = 20 meV (see text).

We show in Fig. 2 the observations mentioned above for LO phonons in GaAs. The measurements were performed in a high purity, LPE-grown sample, with $N_A+N_D \sim 10^{14}$ cm^{-3}. The lower curve (triangles) represents the pure forbidden efficiency, which is obtained for $\hat{e}_L \| \hat{e}_S \| [100]$. The efficiencies for the three configurations can be calculated by using Eqs. (5-6) and the known frequency dependence of a. We obtain the curves displayed in Fig. 3.

The calculated curves reproduce qualitatively the experimental ones. including signs. However, there are at least three important quantitative differences:

a) the calculated interference is stronger than the observed one;
b) in the experimental curve the point of maximum interference is shifted to lower energies with respect to the maximum of the forbidden scattering. This is not reproduced by the calculation.
c) To fit the forbidden LO-resonance, one has to use Eq. (5) with η = 20 meV. This value of the broadening is too large. From the electroreflectance measurements of Aspnes and Studna (Ref. 10), we estimate η = 8 meV for 100 K.

These discrepancies can be partially explained by assuming that part of the forbidden scattering is induced by impurities. The process is indicated in Fig. 1b. The exciton scatters twice: due to the impurity-electron (H_{ie}) and to the electron-phonon (H_{eL}) interaction. The diagram is similar to that for two-phonon scattering. The reason why this higher order process should give a contribution comparable with the "intrinsic" scattering despicted in Fig. 1a is the following: we see from Eq. (5) that the Fröhlich intraband terms lead to a Raman tensor which is proportional to $\vec{q}$. However, in the "intrinsic" case q is determined by the scattering kinematics: $\vec{q} = \vec{k}_L - \vec{k}_S$. $\vec{q}$ is therefore a very small vector. In the case of impurity induced scattering, it is the change of exciton wavevector $\vec{k}$ after the two collisions which has to remain small. Hence, it is possible to excite LO-phonons with larger $\vec{q}$-vectors, thus producing an enhancement of the Fröhlich interaction. We have calculated the intensity of forbidden scattering induced by ionized impurities (Ref. 11). Fig. 4 shows the result for the $E_0+\Delta_0$ gap of GaAs, together with the calculated intrinsic LO-scattering given by Eq. (5). The impurity induced scattering resonates at higher energies, approximately at $\omega_L = E_0+\Delta_0+\hbar\Omega_{LO}$. Instead, Eq. (5) yields a maximum at $E_0+\Delta_0+\hbar\Omega_{LO}/2$. If both, intrinsic and impurity induced scattering are present, the resonance curve for the $z(x,x)\bar{z}$ configuration will have an apparent width which is larger than the individual widths of each contribution. This explains the very large values needed to fit the resonance with Eq. (5) only. On the other hand, the interference will be weaker (point a) and shifted to lower energies (point b), if only the intrinsic part (Eq. (5)) interferes with a. This is indeed the case: the

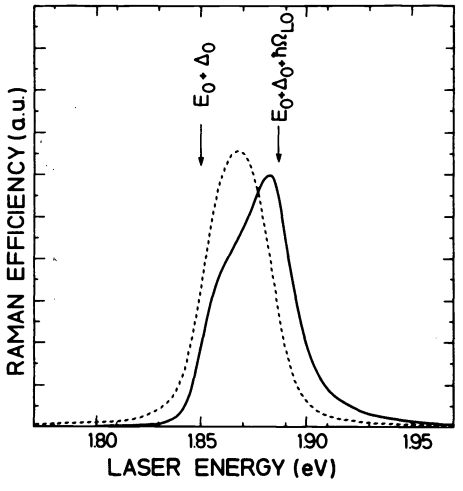

Fig. 4

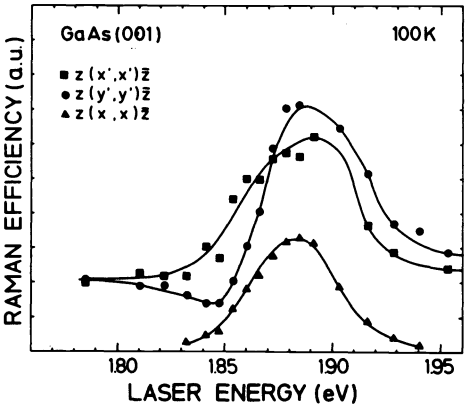

Fig. 5

Fig. 4. Forbidden LO-Raman scattering at the $E_0+\Delta_0$ gap of GaAs. Dashed line: "intrinsic" forbidden LO-scattering, after Eq. (5). Full line: impurity induced forbidden LO-scattering (Ref. 11). The relative scale is arbitrary. The broadening parameter used is η = 8 meV.

Fig. 5. Experimental Raman efficiency for commercial ($N_A + N_D \sim 10^{16}$) GaAs. The notation is the same as in Fig. 2.

deformation potential contribution to forbidden scattering by impurities is negligible, because from the two components of the Hamiltonian H_{el} in Fig. 1b, only the intraband Fröhlich matrix elements are enhanced by the q-vector relaxation. Furthermore, although in principle one has to add all diagrams like 1a and 1b corresponding to one given final state before squaring, 1a and 1b do not interfere because they produce different final states: whereas in diagram 1a phonons with $\vec{q} = \vec{k}_L - \vec{k}_S$ are created, diagram 1b generates phonons with larger q-vector. Hence we can write, instead of Eq. (6):

$$\frac{\partial S}{\partial \Omega} \propto |a \pm a_F|^2 + |a_{F_i}|^2, \qquad (8)$$

where a_F is the impurity induced Raman polarizability. Using Eq. (8) and the calculated $|a_{F_i}|^2$, (Fig. 4), we have plotted in Fig. 2 the interference profiles, assuming that 70% of the forbidden intensity is impurity induced. A good agreement with experiment is obtained, except for an overall shift of $\sim$3+1 meV and a smaller theoretical value for the peak at 1.885 eV in the configuration $z(yy)\bar{z}$. The shift could be understood if one allows for a laser induced heating of the illuminated spot of $\sim$10 K, which is not unreasonable even for a spot produced by a cylindrical lens. Note that the value of η for the fit of the data at 100 K is 8 meV, in reasonable agreement with η = 6 meV found in Ref. 8 at 4 K.

A comparison of our interference results in LPE-grown samples with similar experiments in commercial GaAs ($N_A + N_D \sim 10^{15} - 10^{16}$ cm^{-3}) gives further support to our interpretation in terms of impurity-induced scattering. Fig. 5 shows the results for one of such samples. Note the enhancement of the forbidden scattering efficiency and the weaker interference.

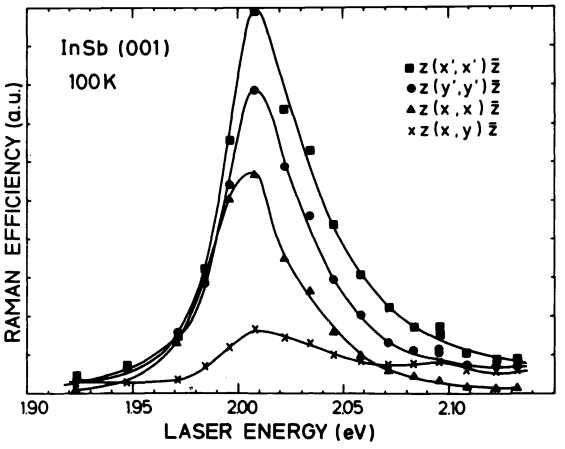

Fig. 6. Experimental Raman efficiency for (001)-InSb. x||[100], y||[010], z||[001], x'||[110], y'||[1$\bar{1}$0]. From Ref. 12.

We show finally in Fig. 6 the experimental results for InSb at the E_1 gap (Ref. 12). In this case both, allowed and forbidden scattering have a resonance behavior (Refs. 6 and 7). However, we do not see strong interference effects because the forbidden LO-scattering is dominated by the impurity mechanism.

REFERENCES

1. H. Riechert et al., Phys. Rev. Lett. 52, 2297 (1984).
2. H.A. Schell, Z. Metalk 48, 158 (1957); H.C. Gatos and M.C. Lavine, J. Electrochem. Soc. 107, 443 (1960).
3. C.Y. Chen, Phys. Rev. B 27, 1436 (1983).
4. J. Menêndez and M. Cardona, Phys. Rev. Lett. 51, 1297 (1983).
5. M. Cardona, Proceedings of the VIIth International Conference on Raman Spectroscopy, Ottawa 1980), W.F. Murphy, editor, p. 14.
6. M. Cardona, Light Scattering in Solids II, ed. by M. Cardona and G. Güntherodt (Springer, Heidelberg, 1982), p. 19.
7. W. Richter, Springer Tracts in Modern Physics 78, p. 121.
8. R.M. Martin, Phys. Rev. B 4, 3676 (1981).
9. R. Zeyher, C.S. Ting, and J.L. Birman, Phys. Rev. B 10, 1725 (1974).
10. D.E. Aspnes and A.A. Studna, Phys. Rev. B 7, 4605 (1973).
11. J. Menêndez and M. Cardona, to be published.
12. J. Menêndez, E. Anastassakis, and M. Cardona (to be published).